

Tuberculosis drugs' distribution and emergence of resistance in patient's lung lesions: A mechanistic model and tool for regimen and dose optimization

N. Strydom¹, S.V. Gupta¹, W.S. Fox¹, L.E. Via², H. Bang², M. Lee³, S. Eum³, T. Shim⁴, C.E. Barry 3rd², M. Zimmerman⁵, V. Dartois⁵, R.M. Savić¹

1. Department of Bioengineering and Therapeutic Sciences, University of California, San Francisco, San Francisco, California, United States of America

2. Tuberculosis Research Section, Laboratory of Clinical Immunology and Microbiology, NIAID, NIH, Bethesda, Maryland, United States of America

3. International Tuberculosis Research Center, Changwon, Republic of Korea

4. Asan Medical Center, Seoul, Republic of Korea

5. Public Health Research Institute and New Jersey Medical School, Rutgers, The State University of New Jersey, Newark, New Jersey, United States of America

Harvard School of Public Health, Unites States

The authors have declared that **no competing interests** exist.

BACKGROUND. The sites of mycobacterial infection in the lungs of tuberculosis (TB) patients have complex structures and poor vascularization, which obstructs drug distribution to these hard-to-reach and hard-to-treat disease sites, further leading to suboptimal drug concentrations, resulting in compromised TB treatment response and resistance development. Quantifying lesion-specific drug uptake and pharmacokinetics (PKs) in TB patients is necessary to optimize treatment regimens at all infection sites, to identify patients at risk, to improve existing regimens, and to advance development of novel regimens. Using drug-level data in plasma and from 9 distinct pulmonary lesion types (vascular, avascular, and mixed) obtained from 15 hard-to-treat TB patients who failed TB treatments and therefore underwent lung resection surgery, we quantified the distribution and the penetration of 7 major TB drugs at these sites, and we provide novel tools for treatment optimization.

METHODS AND FINDINGS. A total of 329 plasma- and 1,362 tissue-specific drug concentrations from 9 distinct lung lesion types were obtained according to optimal PK sampling schema from 15 patients (10 men, 5 women, aged 23 to 58) undergoing lung resection surgery (clinical study NCT00816426 performed in South Korea between 9 June 2010 and 24 June 2014). Seven major TB drugs (rifampin [RIF], isoniazid [INH], linezolid [LZD], moxifloxacin [MXF], clofazimine [CFZ], pyrazinamide [PZA], and kanamycin [KAN]) were quantified. We developed and evaluated a site-of-action mechanistic PK model using nonlinear mixed effects methodology. We quantified population- and patient-specific lesion/plasma ratios (RPLs), dynamics, and variability of drug uptake into each lesion for each drug. CFZ and MXF had higher drug exposures in lesions compared to plasma (median RPL 2.37, range across lesions 1.26-22.03); RIF, PZA, and LZD showed moderate yet suboptimal lesion penetration (median RPL 0.61, range 0.21-2.4), while INH and KAN showed poor tissue penetration (median RPL 0.4, range 0.03-0.73). Stochastic PK/pharmacodynamic (PD) simulations were carried out to evaluate current regimen combinations and dosing guidelines in distinct patient strata. Patients receiving standard doses of RIF and INH, who are of the lower range of exposure distribution, spent substantial periods (>12 h/d) below effective concentrations in hard-to-treat lesions, such as caseous lesions and cavities. Standard doses of INH (300 mg) and KAN (1,000 mg) did not reach therapeutic thresholds in most lesions for a majority of the population. Drugs and doses that did reach target exposure in most subjects include 400 mg MXF and 100 mg CFZ. Patients with cavitory lesions, irrespective of drug choice, have an increased likelihood of subtherapeutic concentrations, leading to a higher risk of resistance acquisition while on treatment. A limitation of this study was the small sample size of 15 patients, performed in a unique study population of TB patients who failed treatment and underwent lung resection surgery. These results still need further exploration and validation in larger and more diverse cohorts.

CONCLUSIONS. Our results suggest that the ability to reach and maintain therapeutic concentrations is both lesion and drug specific, indicating that stratifying patients based on disease extent, lesion types, and individual drug-susceptibility profiles may eventually be useful for guiding the selection of patient-tailored drug regimens and may lead to improved TB treatment outcomes. We provide a web-based tool to further explore this model and results at <http://saviclab.org/tb-lesion/>.

І ЗАРУБІЖНИЙ ДОСВІД

Статтю опубліковано в журналі PLoS Medicine («Публічна наукова бібліотека – Медицина») у квітні 2019 р.; 16 (4): e1002773. Опубліковано онлайн 2 квітня 2019 р. Цифровий ідентифікатор об'єкта (doi): 10.1371/journal.pmed.1002773

Розподіл протитуберкульозних препаратів і поява резистентності в пацієнтів із легеневиими вогнищами: механістична модель та інструмент для оптимізації дози і схеми лікування

Н. Страйдом (N. Strydom)¹, С.В. Гупта (S.V. Gupta)¹, В.С. Фокс (W.S. Fox)¹, Л.І. Віа (L.E. Via)², Г. Бенг (H. Bang)², М. Лі (M. Lee)³, С. Юм (S. Eum)³, Т. Шим (T. Shim)⁴, К.І. Баррі третій (C.E. Barry 3rd)², М. Циммерман (M. Zimmerman)⁵, В. Дартуа (V. Dartois)⁵, Р.М. Савич (R.M. Savic)⁴

1. Кафедра біоінженерії та терапевтичних наук, Каліфорнійський університет, м. Сан-Франциско, Каліфорнія, США
 2. Відділ досліджень туберкульозу, Лабораторія клінічної імунології та мікробіології, Національний інститут алергії та інфекційних захворювань, Національний інститут здоров'я, м. Бетесда, Меріленд, США
 3. Міжнародний центр дослідження туберкульозу, м. Чхангвон, Республіка Корея
 4. Медичний центр Асан, м. Сеул, Республіка Корея
 5. Науково-дослідний інститут громадського здоров'я та Медична школа Нью-Джерсі, Ратгерський університет (Державний університет Нью-Джерсі), м. Ньюарк, Нью-Джерсі, США
- Гарвардська школа громадського здоров'я, США
- Автори не мають конфлікту інтересів.

АКТУАЛЬНІСТЬ РОБОТИ. Вогнища мікобактеріальної інфекції в пацієнтів із туберкульозом легень (ТБЛ) мають складну структуру та погану васкуляризацію, що перешкоджає розподілу лікарських препаратів у цих важкодоступних і стійких до лікування вогнищах, призводить до субоптимальної концентрації препаратів і зрештою зменшує відповідь на терапію та сприяє розвитку резистентності. Кількісна оцінка вогнищового захоплення і фармакокінетики лікарських препаратів у хворих на туберкульоз необхідна для оптимізації схем лікування в усіх вогнищах інфекції, ідентифікації пацієнтів із ризиком резистентності, підвищення ефективності наявних терапевтичних схем і розробки нових. Використовуючи дані щодо концентрації препаратів у плазмі та легеневиих вогнищах 9 різних типів (васкулярних, аваскулярних і змішаних), отриманих від 15 пацієнтів із ТБЛ, які були резистентними до медикаментозної терапії і через це перенесли резекцію легені, ми кількісно визначили розподіл і проникність 7 основних протитуберкульозних препаратів у цих вогнищах, а також розробили новий інструмент для оптимізації лікування.

МЕТОДИ ТА РЕЗУЛЬТАТИ. Від 15 пацієнтів (10 чоловіків і 5 жінок віком від 23 до 58 років), які перенесли резекцію легені, за допомогою оптимальної схеми фармакокінетичного відбору були отримані 329 плазми- та 1362 тканиноспецифічні концентрації препаратів у легеневиих вогнищах 9 типів (клінічне дослідження NCT00816426, проводилося у Південній Кореї в період із 9 червня 2010 р. по 24 червня 2014 р.). Концентрації визначали для 7 основних протитуберкульозних препаратів: рифампіну, ізоніазиду, лінезоліду, моксифлоксацину, клофазиміну, піразинаміду та канаміцину. За допомогою методу нелінійних змішаних ефектів ми розробили та оцінили вогнищово-специфічну механістичну фармакокінетичну модель. Були кількісно оцінені популяційно- та пацієнт-специфічні співвідношення концентрацій у вогнищі та плазмі (RPL), динаміка та варіабельність захоплення кожного препарату у вогнища різних типів. Клофазимін і моксифлоксацин мали вищу експозицію у вогнищах порівняно з плазмою (медіана RPL 2,37, діапазон у різних вогнищах 1,26-22,03); рифампін, піразинамід і лінезолід продемонстрували помірну, хоча й субоптимальну, проникність у вогнища (медіана RPL 0,61; діапазон 0,21-2,4), натомість ізоніазид і канаміцин показали погану тканинну проникність (медіана RPL 0,4; діапазон 0,03-0,73). Для оцінки наявних комбінованих схем лікування та рекомендацій щодо дозування в різних групах пацієнтів було виконано стохастичну фармакокінетично-фармакодинамічну симуляцію. У пацієнтів, які отримували рифампін та ізоніазид і належали до нижнього діапазону розподілу експозиції, протягом значного періоду (>12 год/добу) концентрації препаратів у важковилікованих вогнищах (як-от казеозні вогнища та порожнини) були нижчі за ефективні. Стандартні дози ізоніазиду (300 мг) і канаміцину (1000 мг) не досягали терапевтичних меж у більшості вогнищ для більшості пацієнтів. Цільової експозиції в більшості пацієнтів також не досягли моксифлоксацин 400 мг та клофазимін 100 мг. Пацієнти з порожнинними вогнищами, незалежно від обраного препарату, мали підвищену імовірність субтерапевтичних концентрацій та, відповідно, більш високий ризик розвитку резистентності до лікування. Обмеженням дослідження є невеликий розмір вибірки (15 пацієнтів) та її певна особливість (пацієнти, які перенесли хірургічну резекцію легені через резистентність до медикаментозного лікування). Отримані результати потребують подальшого вивчення і валідації у більших за кількістю та більш різноманітних когортах пацієнтів.

ВИСНОВКИ. Результати дослідження свідчать, що здатність досягати й підтримувати терапевтичні концентрації для кожного типу вогнища і кожного препарату є різною. Отже, стратифікація пацієнтів залежно від поширеності хвороби, типу вогнищ й індивідуального профілю чутливості до лікарських препаратів може допомогти в персоналізованому виборі схеми терапії та зрештою покращити результати лікування туберкульозу. Для подальшого вивчення цієї моделі та отриманих результатів ми розробили онлайн-інструмент, доступний на: <http://saviclab.org/tb-lesion/>.

■ ЗАРУБІЖНИЙ ДОСВІД

Резюме від авторів

Чому було проведено це дослідження?

- Туберкульоз залишається провідною причиною смерті від інфекційних захворювань, і в багатьох пацієнтів лікування є не ефективним, попри застосування комбінованих схем.
- Вірогідною причиною субоптимальної відповіді є знижена проникність лікарського препарату у різні сформовані імунною системою людини легеневі вогнища, у яких мікобактерії залишаються у відокремлених місцях, не доступних для препарату.

Що дослідники зробили і які отримали результати?

- Використовуючи фактичні дані пацієнтів, ми розробили математичну модель для 7 основних протитуберкульозних препаратів, що описує рівень і швидкість проникнення препарату в 9 різних туберкульозних вогнищ, у яких перебувають мікобактерії.
- Більшість протитуберкульозних препаратів виявили погану проникність у порожнинні вогнища, що призводить до неадекватних концентрацій препарату у місці хвороби.
- Симуляція, проведена з метою пошуку оптимальних комбінацій препаратів для вилікування у місці інфекції, показала, що комбінації клофазимін + моксифлоксацин та клофазимін + лінезолід є оптимальними для пацієнтів із казеозними вогнищами.

Що означають ці результати?

- Протитуберкульозні препарати мають неоднакову проникність у різні тканини. З огляду на те, що кожен хворий на туберкульоз є унікальним стосовно типів вогнищ і легеневої патології, теперішній підхід «одна схема для всіх пацієнтів» не можна вважати адекватним.
- З метою максимізації частоти вилікування пацієнта необхідний персоналізований підхід, у якому вибір оптимального препарату для конкретного хворого базується на клінічному фенотипі.

Статья опубликована в журнале PLoS Medicine («Публичная научная библиотека – Медицина») в апреле 2019 г.; 16 (4): e1002773. Опубликовано онлайн 2 апреля 2019 г. Цифровой идентификатор объекта (doi): 10.1371/journal.pmed.1002773

Распределение противотуберкулезных препаратов и появление резистентности у пациентов с легочными очагами: механистическая модель и инструмент для оптимизации дозы и схемы лечения

Н. Страйдом (N. Strydom)¹, С.В. Гупта (S.V. Gupta)¹, В.С. Фокс (W.S. Fox)¹, Л.И. Виа (L.E. Via)², Г. Бэнг (H. Bang)², М. Ли (M. Lee)³, С. Юм (S. Eum)³, Т. Шим (T. Shim)⁴, К.И. Барри третий (C.E. Barry 3rd)², М. Циммерман (M. Zimmerman)⁵, В. Дартуа (V. Dartois)⁵, Р.М. Савич (R.M. Savic)¹

1. Кафедра биоинженерии и терапевтических наук, Калифорнийский университет, г. Сан-Франциско, Калифорния, США
 2. Отдел исследований туберкулеза, Лаборатория клинической иммунологии и микробиологии, Национальный институт аллергии и инфекционных заболеваний, Национальный институт здоровья, г. Бетесда, Мэриленд, США
 3. Международный центр исследования туберкулеза, г. Чхангвон, Республика Корея
 4. Медицинский центр Асан, г. Сеул, Республика Корея
 5. Научно-исследовательский институт общественного здоровья и Медицинская школа Нью-Джерси, Ратгерский университет (Государственный университет Нью-Джерси), г. Ньюарк, Нью-Джерси, США
- Гарвардская школа общественного здоровья США
Авторы **не имеют конфликта интересов.**

АКТУАЛЬНОСТЬ. Очаги микобактериальной инфекции у пациентов с туберкулезом легких (ТБЛ) имеют сложную структуру и плохую васкуляризацию, что препятствует распределению лекарственных препаратов в этих труднодоступных и устойчивых к лечению очагах, приводит к субоптимальной концентрации препаратов и в итоге уменьшает ответ на терапию и способствует развитию резистентности. Количественная оценка очагового захвата и фармакокинетики лекарственных препаратов у больных туберкулезом необходима для оптимизации схем лечения во всех очагах инфекции, идентификации пациентов с риском резистентности, повышения эффективности имеющихся терапевтических схем и разработки новых. Используя данные о концентрации препаратов в плазме и легочных очагах 9 различных типов (васкулярных, аваскулярных и смешанных), полученных от 15 пациентов с ТБЛ, которые были резистентными к медикаментозной терапии и поэтому перенесли резекцию легкого, мы количественно установили распределение и проницаемость 7 основных противотуберкулезных препаратов в этих очагах, а также разработали новый инструмент для оптимизации лечения.

ЗАРУБІЖНИЙ ДОСВІД

МЕТОДИ И РЕЗУЛЬТАТЫ. От 15 пациентов (10 мужчин и 5 женщин в возрасте от 23 до 58 лет), перенесших резекцию легкого, с помощью оптимальной схемы фармакокинетического отбора были получены 329 плазмо- и 1362 тканеспецифические концентрации в легочных очагах 9 типов (клиническое исследование NCT00816426, проводилось в Южной Корее в период с 9 июня 2010 г. по 24 июня 2014 г.). Концентрации определяли для 7 основных противотуберкулезных препаратов: рифампина, изониазида, линезолида, моксифлоксацина, клоfazимина, пиразинамида и канамицина. С помощью метода нелинейных смешанных эффектов мы разработали и оценили очагово-специфическую механистическую фармакокинетическую модель. Были количественно оценены популяционно- и пациент-специфические соотношения концентраций в очаге и плазме (RPL), динамика и вариабельность захвата каждого препарата в очагах различных типов. Клоfazимин и моксифлоксацин имели более высокую экспозицию в очагах по сравнению с плазмой (медиана RPL 2,37, диапазон в различных очагах 1,26-22,03); рифампин, пиразинамид и линезолид продемонстрировали умеренную, хотя и субоптимальную, проницаемость в очаги (медиана RPL 0,61, диапазон 0,21-2,4), тогда как изониазид и канамицин показали плохую тканевую проницаемость (медиана RPL 0,4, диапазон 0,03-0,73). Для оценки имеющихся комбинированных схем лечения и рекомендаций относительно дозирования в различных группах пациентов была выполнена стохастическая фармакокинетически-фармакодинамическая симуляция. У пациентов, получавших рифампин и изониазид и относящихся к нижнему диапазону распределения экспозиции, на протяжении значительного периода (>12 ч/сут) концентрации препаратов в трудноизлечимых очагах (например, казеозные очаги и полости) были ниже эффективных. Стандартные дозы изониазида (300 мг) и канамицина (1000 мг) не достигали терапевтического порога в большинстве очагов для большинства пациентов. Целевой экспозиции у большинства пациентов также не достигли моксифлоксацин 400 мг и клоfazимин 100 мг. Пациенты с полостными очагами, независимо от выбранного препарата, имели повышенную вероятность субтерапевтических концентраций и, соответственно, более высокий риск развития резистентности к лечению. Ограничениями исследования являются небольшой размер выборки (15 пациентов) и ее уникальность (пациенты, перенесшие хирургическую резекцию легкого вследствие резистентности к медикаментозному лечению). Полученные результаты требуют дальнейшего изучения и валидации в больших по количеству и более разнообразных когортах пациентов.

Выводы. Результаты исследования свидетельствуют о том, что способность достигать и поддерживать терапевтические концентрации для каждого типа очага и каждого препарата существенно отличается. Таким образом, стратификация пациентов в зависимости от распространенности болезни, типа очагов и индивидуального профиля чувствительности к лекарственным препаратам может помочь в персонализированном выборе схемы терапии и в итоге улучшить результаты лечения туберкулеза. Для дальнейшего изучения этой модели и полученных результатов мы разработали онлайн-инструмент, доступный на: <http://saviclab.org/tb-lesion/>.

Introduction

A primary objective of contemporary tuberculosis (TB) drug development programs is the identification of therapeutic regimens that have shorter treatment duration and improved efficacy with decreased risk of resistance [1]. Similarly, therapeutic use of the current regimen for drug-sensitive (DS)-TB can further be optimized, as its current use, despite high efficacy of the regimens (>95 %) in the clinical trials, leads to unsatisfying effectiveness in the field and emergence of resistance [2-4]. Further, both efficacy and effectiveness of regimens for all forms of drug-resistant TB can further be optimized to reach high cure rates. A significant barrier to improving TB regimens is the complex pathology of TB in human lung tissue. Drug access to the site of mycobacterial infection becomes increasingly difficult as the disease progresses from initial macrophage infection to the formation of heterogeneous granuloma lesions that have variable or limited blood supply [5, 6]. In a clinical research study of drug distribution into TB lesions [7], imaging and conventional mass spectrometry of resected lung lesions from patients with multidrug-resistant (MDR)-TB showed that the distribution patterns of TB drugs within these diverse lesions vary significantly and that, in many cases, drug concentrations in lesions correlate poorly with concentrations measured in blood [7, 8]. Presence of cavitary lesions and extensive lung pathology has been established as a major risk factor for poor TB outcomes, which could

be explained by reduced drug penetration at these sites. Recent translational studies of rifapentine's poor penetration properties in the cavitary lesions quantitatively predicted and explained substantially longer times of culture conversion observed in patients with large cavitation and comparably high blood exposures [9, 10]. Drug regimens designed solely based on plasma pharmacokinetic (PK) profiles are therefore inadequate to predict the true sterilizing effect of drugs at the site of mycobacterial infection, especially for the drugs that have reduced or variable penetration at the site of infection. Additionally, mycobacterial resistance may be driven by this differential drug exposure in infected TB lesions, for which windows of monotherapy at selected times and locations likely increase drug pressure. Our goal is to provide a data-driven framework and tool that enables quantification of lesion-specific information in addition to dosing regimens and microbiological PK/pharmacodynamic (PD) parameters and can serve the TB community at multiple levels, such as a) treatment optimization to achieve cure, b) profiling high-risk populations based on reduced penetration in hard-to-treat lesions with the current regimens, and c) in silico investigation and optimization of novel regimens that achieve sterilization and prevent resistance development.

Here, (1) to our knowledge, we report for the first time the penetration of kanamycin (KAN) and linezolid (LZD) in human TB lesions; (2) we report a population lesion-focused PK model and parameters from the observed concentration-time

■ ЗАРУБІЖНИЙ ДОСВІД

profiles in TB patients of first-line drugs isoniazid (INH), rifampicin (RIF), and pyrazinamide (PZA) and second-line drugs moxifloxacin (MXF), KAN, clofazimine (CFZ), and LZD in 9 distinct human lesion-specific tissues: uninvolved lung, closed nodules (cellular, necrotic, or fibrotic), cavity wall, cavity caseum or nodule caseum, and fungal ball; (3) we profile by means of stochastic population simulations the clinical utility of these 7 drugs within a regimen with a focus on identifying underexposed lesions, suboptimal doses and regimens, and patient subgroups at risk of relapse and resistance development; and (4) we provide a tool that can be used by scientific and clinical communities to evaluate the lesion-focused time course of drug levels following various drug combinations, doses, and schedules.

Methods

Patient, drug regimen, and surgical procedure details

Original clinical trial design and partial raw data on RIF, INH, PZA, CFZ, and MXF in plasma, lung tissue, and lesions of TB patients were previously reported in Prideaux and colleagues, and these data were added to our database. Briefly, 15 patients who failed initial TB treatment and who were receiving selected first- and second-line TB drugs underwent elective lung resection surgery to debulk tubercular lung disease at the National Masan TB Hospital and Asan and Samsung Medical Center in Seoul and Pusan National University Hospital in Pusan, Republic of Korea. The study was approved by the Institutional Review Board of the National Institute of Allergy and Infectious Diseases and by the institutional review boards of the hospitals conducting the study in the Republic of Korea. The subjects gave written informed consent to participate in the study and to have their resected tissue used for research. Exclusion criteria included patients younger than 20, women pregnant or unwilling to avoid pregnancy, and HIV positive. All patients received single-dose tablets of 600 mg RIF, 300 mg INH, 1,500 mg PZA, 400 mg MXF, and 1,000 mg KAN dissolved in 5 ml normal saline (0.9 % NaCl) before their scheduled surgery. Patients taking LZD and CFZ as part of their background regimens were considered at steady state if they had been on the drugs for more than 14 days. Patients receiving other drugs that were not the approved study drugs, such as LZD and CFZ, were not given these drugs on the day of surgery to minimize drug–drug interactions. These background drugs were still quantified and included in the data set analyzed and modeled in the present work, including appropriate dosing histories that had the exact times of their previous LZD and CFZ dose, which occurred more than 24 h before surgery. The lower limits of quantification (LOQ) were 1 ng/mL in plasma and 10 ng/g in tissue for both CFZ and LZD. Individual patient dosing times were planned to occur at approximately 2, 4, 8, 12, or 24 h before surgery with the aim of collecting longitudinal tissue sample concentrations. Plasma samples were drawn prior to and at the time of surgery. The PK sampling times served as proposed times, and no interference to the surgery occurred to obtain exact PK times. The drug administration was timed to occur before the surgery at various time points so different patients could contribute lesion samples at different time points post dose to reconstruct the entire PK profile. The exact resection times were recorded, and collected lung tissues were

classified and dissected into defined lesions by macroscopic appearance and flash frozen for drug quantification. During resection, the pulmonary artery was clamped and resected tissue very briefly rinsed to avoid blood contamination in the tissue. Samples were further classified by histological and radiological methods into lung, necrotic nodule, caseum from closed nodule, caseous fibrotic nodule, caseum from cavity, cavity wall, fibrotic tissue, small nodule, and fungal ball, quantified by HPLC-coupled tandem mass spectrometry (LC/MS-MS), and imaged by matrix-assisted laser desorption-ionization mass spectrometry imaging (MALDI-MSI). For large enough lesions that had discrete necrotic content, the lesion walls and caseum were analyzed separately.

Plasma PK models

Plasma compartmental models were built for each drug based on established methodology. To capture the absorption, distribution, and clearance of the drugs, 1- and 2-compartment models with first-order elimination, parameterized in terms of oral clearance (CL), oral volume of distribution (V), peripheral volume of distribution (V2), and intercompartmental clearance accounting for drug movement between central and peripheral volume of distribution (Q), were tested and fitted to the data. To describe the process of absorptions, different established models were explored for the absorption profile of the drugs: a straight forward first-order model and, if necessary, a lag time and a transit compartment model with a fixed or estimated number of compartments were evaluated [11, 12]. Within a population, we expect variability in some PK parameters, and to account for this distribution, interindividual variability (IIV) parameter was tested on plasma PK parameters and allowed based on the magnitude of estimates and the likelihood ratio test (LRT), which acts as a measure of statistical significance.

The plasma PK model for PZA, MXF, KAN, CFZ, and LZD was a 1-compartment model with first-order absorption described by the following equation:

$$\frac{dA}{dt} = k_a \times A_1 - \left(\frac{CL}{V}\right) \times A_2, \quad (1)$$

in which A1 is the amount of drug in the absorption compartment, A2 is the amount of drug in the central compartment in milligrams, CL is the clearance in liters per hour, and V is the volume of distribution in liters.

in which A1 is the amount of drug in the absorption compartment, A2 is the amount of drug in the central compartment in milligrams, CL is the clearance in liters per hour, and V is the volume of distribution in liters.

RIF PKs were described with a 1-compartment model linked to the transit compartment absorption chain, as described in Savic and colleagues [12], while the INH model was a 2-compartment model with first-order absorption.

Tissue penetration model

Penetration of each drug into lung and lesions was described using a separate lesion compartment, as described by Kjellsson and colleagues [13], according to the following equations:

$$\frac{dC_{lung}}{dt} = k_{pl-lung} \times (R_{lung-pt} \times \frac{A_{plasma}}{V_{plasma}} - C_{lung}), \quad (2)$$

■ ЗАРУБІЖНИЙ ДОСВІД

$$\frac{dC_{lesion}}{dt} = k_{pl-lesion} \times (R_{lesion-pl} \times \frac{A_{plasma}}{V_{plasma}} - C_{lesion}), \quad (3)$$

in which C_{lung} and C_{lesion} represent the drug concentration within uninvolved lung and lesion, $K_{pl-lung}$ and $K_{pl-lesion}$ are intercompartment rate constants for the transfer of drug from the plasma to lung or lesion, $R_{lung-pl}$ and $R_{lesion-pl}$ are the penetration coefficients (ratios) between lung or lesion and plasma, and A_{plasma}/V_{plasma} is the drug concentration in plasma at time t . If the ratio value is 1, there is equal distribution between plasma and tissue; if the ratio is <1 , there is reduced drug penetration from plasma to the tissue, and if the ratio is >1 , there is accumulation of drug in the tissue compared to the plasma.

Population PK model selection and evaluation

Concentration–time data for each drug in plasma, lesions, and uninvolved lung from each patient were modeled using a population PK methodology, which is the appropriate method for sparse longitudinal data with expected variability between patients and separation of the signal from noise due to random error. To best fit the sparse longitudinal data, we used nonlinear mixed-effects models with first-order conditional estimation methods as implemented in the software NONMEM (version 7.3; ICON Development Solutions, Ellicott City, MD, United States). Graphical, statistical, and exploratory analyses were conducted using the open-source software R (version 3.3.1). The Xpose (version 4.0) package, implemented within R, was used for graphical evaluations and visual predictive checks [14].

A stepwise approach was taken to model fitting. First, a structural PK model was fit to the plasma PK data, which contained the longitudinal samples in each patient, required to describe the population distribution. After establishing and validating the plasma PK model, PK data in uninvolved-lung and individual-lesion subtypes were added one lesion at a time, and the model was expanded in a stepwise manner, followed by assessment of parameters and goodness of fit. The plasma/lesion ratios and rates of drug uptake into the lesion compartments were estimated. It was assumed that the drug distribution into the lesion can only happen from the plasma, given general physiological knowledge of drug distribution. To account for accumulation of drugs into the lesions for patients at steady state, the lesion compartments were never reset after the dosing. To account for potential noise in the data, additive and proportional error models of residual variability were explored. Different residual errors were estimated for plasma, lung, and lesions. The LRT was used to evaluate statistical significance for inclusion of additional parameters in the nested models, with a decrease of 3.84 points (proportional to $-2 \log$ likelihood change), considered statistically different with 5 % significance level assuming the LRT is χ^2 distributed. No additional variability was added to the lesion parameters, as the data were too sparse with a single-time point per patient. The variance seen for the lesion PKs follows expected plasma variance.

Finally, individual and population predictions of exposures at steady state were estimated in terms of the

area under the concentration–time curve over 24 h at steady state (AUC₀₋₂₄) and peak concentration (C_{max}) in plasma, lung, and each lesion subtype. Simulations achieved 2 goals: (1) evaluation of the performance properties of selected models (visual predictive checks) and (2) exploration of PKPD relationships with alternative dosing scenarios.

PK/PD exposure target selection

Antibiotic exposure to determine effective activity can be quantified using PK/PD indices: area under the concentration curve (AUC), maximum concentration (C_{max}), and time, all relative to minimum inhibitory concentration (MIC). The final population PK parameters and interindividual variability were used to simulate PK profiles over the course of the treatment. Distributions of wild-type MIC were obtained from published epidemiological data based on clinical isolates tested according to standardized EUCAST/CLSI methodology as well as literature [15, 16]. Target attainment analyses were performed using the upper limit of the published wild-type MIC distributions for each drug. Target analysis was not possible for PZA due to the drug's apparent lack of antimycobacterial activity in vitro under standardized pH-acidic conditions. All simulations were performed using the `mlxR` package in R, with the final estimates and patient distribution from the established clinical PK model [17, 18].

Implementation of the model into interactive tool

A user interface to allow rapid simulations of the described lesion model and predict new data based on dosing regimen, microbiology values, and patient distribution was developed using the Shiny package from Rstudio [19, 20]. The web application utilized the `mlxR` package for calculating and running the population model [17]. The code used is available within the web application and can be found at <http://saviqlab.org/tb-lesion/>.

Results

Subject demographics and observed PK profiles

Previously described clinical study NCT00816426 collected lung lesion samples after elective lung resection from 10 male and 5 female patients aged 23 to 58 who failed TB treatment [7]. The demographics of the individual patients and their respective steady-state drugs are presented in Table 1. The PK data collected included samples from uninvolved lung, necrotic nodule, caseum from closed nodule, caseous fibrotic nodule, caseum from cavity, cavity wall, fibrotic tissue, small nodule, and fungal ball over a time range of 3–33 h, and plasma samples were taken prior to and at the time of surgery, with a total of 329 plasma and 1,362 lesion data points above LOQ included in the analysis. Drug concentrations differed greatly among lesions and patients and even within similar lesions of a single patient, demonstrating the high variance of TB drug distribution into lung lesions. Plasma and lesion concentrations of KAN and LZD are reported here for the first time, as well as spatial distribution of LZD and CFZ as measured by two-dimensional MALDI-MSI. We observe that LZD seems to distribute equally between caseum and cellular tissue, suggesting high penetration into caseum. In contrast, CFZ shows little penetration into the caseum region and has a much higher affinity for cellular tissues surrounding the caseum area.

ЗАРУБІЖНИЙ ДОСВІД

Table 1. Patient demographics

Subject	Gender	Age (yrs)	BMI (kg/m ²)	Prior TB episodes	Study steady-state drugs	Other steady-state drugs	NAT2 Polymorph (phenotype [§])
1	Male	27	24.0	2	MFX, KAN	LZD, AUG, CLA	NAT2*4 (Fast)
2	Male	51	22.3	1	-	LFX	NAT2*4 (Fast)
3	Male	40	17.3	2	INH	EMB	NAT2*4 (Fast)
4	Female	53	22.0	8	-	-	[¥] NAT2*6A (Intermediate)
5	Male	54	29.4	2	-	LZD, AMK, PAS, CFZ	NAT2*4 (Fast)
6	Female	48	22.2	1	MFX	LZD, CS, AMX, PTH	NAT2*4 (Fast)
7	Male	43	27.1	2	MFX, KAN	LZD, PAS, AUG	NAT2*4 (Fast)
8	Male	59	19.2	1	-	-	NAT2*6 A (Slow)
9	Male	36	24.8	1	MFX, KAN, PZA	LZD, CS, PAS, PTH	NAT2*4 (Fast)
10	Female	23	18.8*	2	-	LZD, CS, CFZ	[¥] NAT2*7B (Intermediate)
11	Male	47	18.9	1	INH	LZD, CS, AUG, PTH, STM	NAT2*4 (Fast)
12	Male	39	22.2	4	PZA	CS, LFX, PTH, STM	NAT2*4 (Fast)
13	Female	58	21.2	1	KAN	LZD, CS, PAS	NAT2*4 (Fast)
14	Female	27	20.0	1	PZA	LZD, CS, AUG, STM	NAT2*4 (Fast)
15	Male	44	24.1	1	INH, PZA	EMB, LFX	NAT2*6A (Slow)

Abbreviations: AMK, amikacin; AUG, amoxicillin/clavulanate; CFZ, clofazimine; CLA, clarithromycin; CS, cycloserine; EMB, ethambutol; INH, isoniazid; KAN, kanamycin; LFX, levofloxacin; LZD, linezolid; MFX, moxifloxacin; NAT2, N-acetyltransferase 2; PAS, para-aminosalicylate; PTH, prothionamide; PZA, pyrazinamide; RIF, rifampicin; STM, streptomycin.

*Patient received LZD 450-mg dose due to low BMI.

[§]Acetylase phenotype inferred from NAT2 genotype.

[¥]Heterozygous allele.

Plasma and tissue PK model

The structural model describing the plasma PKs and distribution of RIF, INH, PZA, MFX, KAN, LZD, and CFZ in the 9 lung tissue compartments was used. A 1-compartment model with first-order absorption best described the plasma data of PZA, MFX, KAN, LZD, and CFZ. RIF model-building required a transit absorption compartment to capture the observed absorption data, and INH PKs best fit a 2-compartment model with first-order absorption and lag time. INH undergoes N-acetyltransferase 2 (NAT2) mediated conversion to acetyl-INH in the liver. Due to widespread genetic polymorphisms in NAT2 and a demonstrated correlation between polymorphism and INH concentration-time profile [21], INH profiles were characterized for slow, intermediate, and fast acetylators with 11 out of the 15 subjects phenotyped as fast acetylators, i. e., high metabolizers. Further discussion, therefore, focuses on fast acetylators and their increased risk of treatment failure. Established models were evaluated by a visual predictive check of the final model, stratified by drug and lesion, shown in simplified The final estimates of the parameter values from the plasma PK models are shown in Table 2. Clearance values for all drugs except INH were within reported literature ranges, showing that this subpopulation of patients exhibits similar PK profiles to the general population. Tissue distribution was best described by separate compartment with 2 distinct parameters: parameter to describe the rate of drug movement from plasma to each lesion type or

compartment (KPL) and a parameter to estimate the ratio of drug concentration observed in the tissue compared to the concentration in plasma (RPL). Table 3 shows the final estimated penetration ratios of each drug in the 9 types of lung and lesion compartments.

Rifampin

Overall, RIF distributed reasonably well into all lesion subtypes and compartments, with penetration ratios ranging from 0.3 to 0.7. RIF concentrations were below the MIC for less than 50% of the dosing interval in all tissue compartments in typical patients. Only one patient had received multiple RIF doses, limiting the possibility to establish steady-state residence time in lesions of interest.

Isoniazid

Concentrations of the other first-line drug, INH, were below the MIC for more than 10 h of the dosing interval in the majority of lesion subtypes, except for fungal ball tissue. Comparing tissue-penetration coefficients of INH between lesions, higher penetration was observed in caseum from closed nodules and caseous fibrotic nodules, suggesting more rapid and favorable penetration and affinity in this more difficult-to-treat caseous environment. However, it has been found that INH has no detectable activity against nonreplicating bacilli found in caseum [22], indicating that despite favorable penetration, adequate concentrations are likely not reached in this compartment.

ЗАРУБІЖНИЙ ДОСВІД

Table 2. Plasma PK parameters

Parameter	RIF	INH	PZA	MFX	CFZ	KAN	LZD
Rate of absorption (h ⁻¹)	1.55 (0.0434)	0.738 (0.150)	0.554 (0.183)	1.55 (1.50)	0.100 (0.349)	1.65 (0.066)	2.13 (0.010)
Lag time (h)	-	0.130 (0.230)	-	-	-	-	-
Clearance (L/h)	5.72 (1.44)	s: 9.41 (3.26) i: 24.0 (9.41) f: 38.1 (5.41)	2.05 (0.312)	8.93 (1.50)	16.3 (0.109)	4.61 (0.251)	3.77 (0.082)
Central volume (L)	52.3 (12.5)	48.9 (9.98)	30.0 (2.71)	147 (32.9)	280 (0.273)	30.6 (0.167)	145 (0.530)
Intercomp clearance	-	6.43 (1.86)	-	-	-	-	-
Peripheral volume (L)	-	40.4 (14.3)	-	-	-	-	-

Abbreviations: CFZ, clofazimine; f, fast; i, intermediate; INH, isoniazid; KAN, kanamycin; LZD, linezolid; MFX, moxifloxacin; NONMEM, NONlinear Mixed Effects Modeling; PK, pharmacokinetic; PZA, pyrazinamide; RIF, rifampicin; s, slow.
*Standard error shown in parentheses describes the precision of the parameters generated by NONMEM. INH clearance was estimated for 3 subgroups representing s, i, and f metabolizers.

Table 3. Estimated drug lesion ratios

Drug	Lung	Cavity wall	Small cellular nodule	Caseum from cavity	Closed nodule caseum	Caseous fibrotic nodule	Necrotic nodule	Fibrotic tissue	Fungal ball
RIF	0.694 (0.19)	0.614 (0.16)	0.348 (0.18)	0.449 (0.32)	0.443 (0.25)	0.733 (0.29)	0.569 (0.12)	0.539 (0.18)	0.447 (0.07)
INH	0.552 (1.20)	0.175 (0.80)	0.228	0.298 (0.42)	0.824 (0.04)	0.516 (0.04)	0.376 (0.52)	0.267 (2.79)	3.04 (0.0004)
PZA	0.616 (0.17)	0.72 (0.02)	0.698 (0.04)	0.544 (0.13)	0.394 (0.32)	0.611 (0.032)	0.676 (0.09)	0.607 (0.04)	0.429 (0.001)
MFX	4.41 (2.29)	2.33 (0.77)	1.34 (1.46)	1.26 (0.37)	1.83 (2.24)	2.41 (0.99)	2.29 (1.16)	1.69 (1.46)	2.08 (0.01)
CFZ	12.4 (0.10)	11.3 (3.68)	11.47 (2.55)	1.34 (0.48)	NA	14.3 (0.30)	7.32 (1.38)	22.03 (4.28)	NA
KAN	0.404 (0.61)	0.468 (0.96)	0.422 (1.12)	0.468 (0.13)	0.176 (0.17)	0.503	0.667 (0.46)	0.404 (1.12)	0.918
LZD	0.609 (0.10)	0.497 (0.34)	0.531 (0.24)	0.651 (0.036)	0.673 (0.016)	0.177 (0.073)	0.609 (0.040)	0.487 (0.114)	NA

Abbreviations: CFZ, clofazimine; INH, isoniazid; KAN, kanamycin; LZD, linezolid; MFX, moxifloxacin; NA, not available; PZA, pyrazinamide; RIF, rifampicin.

*Standard error shown in parentheses describes the precision of the parameters.

Pyrazinamide

PZA is considered a treatment-shortening and sterilizing drug and performs best in the acidic environments thought to be present in the phagolysosomes of infected macrophages and in the necrotic foci of closed nodules and cavities [23]. Differentiating lesion subtypes based on their likely pH microenvironments, PZA should be most active in necrotic nodules, macrophage rich lung, cavity wall, cavity caseum, closed nodule caseum, and small cellular nodules. Considering lowered MIC in these lesion compartments, PZA concentrations were above the “acidic” MIC for 9 h of the dosing interval in the caseum of closed nodules and for at least 70% of the dosing interval in lung tissue, cavity wall, cavity caseum, cellular and necrotic nodules, and fibrotic tissue.

Moxifloxacin

Second-line drugs MFX and CFZ (100 mg daily) had the highest lesion-penetrating ratios with higher observed tissue than plasma concentrations. As a result, MFX was above the MIC for the dosing interval in all lesion subtypes, including caseous lesions.

Clofazimine

CFZ had high-penetration ratios into cellular tissues, such as uninvolved lung, cavity wall and small cellular nodules, and fibrotic lesions, translating into concentrations above its MIC for the entire dosing interval. Penetration in tissues with little or no cellularity, such as caseum from cavity, was low relative to other lesions. Thus, CFZ is expected to reach cellular – but not caseous – lesion

■ ЗАРУБІЖНИЙ ДОСВІД

compartments at adequate concentrations, in line with its reduced efficacy in mouse models that present large necrotic lesions [24]. In addition, like INH, CFZ has no detectable activity against nonreplicating bacilli found in caseum [22].

Kanamycin

A 1,000-mg dose of KAN had lower concentrations in tissues compared to plasma and had a very low tissue-to-plasma ratio of 0.176 in caseum from closed nodules. The highest estimated ratio of KAN was in necrotic nodules corresponding to the high C_{max}/MIC and a long time above MIC profile.

Linezolid

The typical profile of 300 mg LZD had best concentration levels and tissue-to-plasma ratios in necrotic foci. Within most of the caseous lesions, LZD concentrations were well maintained above MIC after reaching steady state.

At-risk patients show low target attainment in lesions

Next, the population PK model was implemented as a simulation tool to stratify patients at risk of treatment failure. The population PK parameter estimates in our population corresponded well to reported literature values in general TB patient population; therefore, we assume that this population is similar in its PK profiles to the general population. Considering that 95 % of TB patients are successfully cured at the completion of standard treatment for drug-susceptible TB, we investigated the lower fifth percentile of patient concentration-time profiles in plasma to account for the fraction of the population group that fails treatment. This fifth percentile, was simulated from 1,000 repetitions at steady state for each drug in lesion subtypes. The simulated at-risk population showed that first-line drug concentrations do not stay above the respective MIC for the entire dosing interval. The horizontal timeline bars illustrate the period during which a drug is above or below its MIC within a dosing interval in each of the 9 tissue or lesion types. On average, RIF was below MIC values for hard-to-treat necrotic foci for less than 50 % of the dosing interval in at-risk patients. While INH reached adequate concentrations in fungal ball tissue for the entire dosing interval and in caseous fibrotic nodule for half of the dosing interval, in other lesions, INH was below its MIC more than 75 % of its dosing interval. In at-risk patients, PZA achieved concentrations above the MIC for 38-55 % of the dosing interval in almost all lesion types, with caseum from cavity, closed nodule caseum, and caseous fibrotic nodule showing the longest below-MIC periods, assuming an optimal acidic MIC of 12.5 mg/L in all lesions.

Second-line CFZ achieved adequate exposure in cellular lesion compartments, consistent with its higher intracellular uptake in macrophages and other immune cells. MFX performed better than most drugs in all lesions, and while LZD performed well in all lesions in typical patients, at-risk patients had less than 50 % above-MIC concentrations – except for small cellular nodules. The ratio between peak concentration (C_{max}) and MIC is generally considered the PK/PD driver of aminoglycosides. In at-risk patient populations, the C_{max}/MIC of KAN was approximately 2-fold lower than in patients with standard exposure. Across drugs, closed nodule caseum was the most problematic lesion compartment.

TB drugs do not reach their PK/PD target in all lesions

For most TB drugs, the exposure/potency index that drives efficacy is the ratio of the area under the concentration curve to the MIC (AUC_{0-24}/MIC). Published AUC_{0-24}/MIC ratios – associated with 90 % maximal effective concentrations (EC_{90}) – used in the present simulations were 1,360 for RIF, 567 for INH, 56 for MFX, and 25 for LZD [15,16,25,26]. Aminoglycosides, like KAN, generally show C_{max} -dependent killing, and a C_{max}/MIC value greater than 10 is thought to result in 90 % killing in the treatment of pneumonia [27]. In the absence of experimental and clinical data for CFZ, 90 % time above MIC was chosen as the PK/PD index.

The simulation consisted of 1,000 patients and showed improved outcomes for MFX and RIF, but INH and KAN performed poorly across lesions, with only a small fraction of the patient population reaching target breakpoints of efficacy. CFZ performed well across all lesion types except caseum from cavity.

Simulations can guide the selection of the best multidrug options for patients with cavitary lesions

Overall, the plasma and lesion PK data collected in this study clearly highlight the impact of interindividual PK variability and differential lesion penetration on PK/PD target attainment. Importantly, the simulations uncover the potential for actual monotherapy in specific lesion compartments where several drugs in the regimen do not reach adequate concentrations, creating windows of opportunity for the development of resistance in patients with low exposure (Fig 1). The first-line regimen (RIF-INH-PZA) performed poorly in cavity and closed nodule caseum, with only a maximum of 2 drugs with suitable drug levels in each lesion and sufficient windows of monotherapy that could lead to resistance. Collectively, the second-line drugs exhibited limited time above MIC in cavity caseum.

Using the PK/PD indices described in the previous section, we calculated the percentage target attainment of each drug in each lesion type to identify regimens that would be effective in specific lesions (Fig 1). Worst outcomes were predicted in cavity caseum and closed nodules, with only RIF, MFX, and LZD reaching effective concentrations. First-line drug RIF outperformed INH, which seldom impacted the population percentage reaching PK/PD targets. CFZ exhibited a contrasted profile, achieving high population percentages of target attainment in cellular lesions while not contributing to efficacy in caseum. KAN did not meet expectations and could benefit from dose optimization to ensure that lesion concentrations are adequate to inhibit bacteria; however, KAN's severe safety profile would limit such optimization.

To further examine if the drugs could perform better at increased doses, dose-escalation simulations of 600 mg and 800 mg MFX were performed but did not produce significant changes in outcome. High-RIF doses of 900 mg or 1,200 mg predicted 100 % target attainment in the simulated population. Simulated LZD doses of 600 mg twice daily and 1,200 mg daily showed improved efficacy outcomes almost 2-fold. Considering LZD toxicity is concentration driven, a 600-mg twice-daily dose would decrease risk of toxicity while still maintaining AUC values similar to a 1,200 mg daily dose [28]. To account for the phenotypic drug tolerance of *Mycobacterium tuberculosis* (Mtb) bacilli in nodule and

ЗАРУБІЖНИЙ ДОСВІД

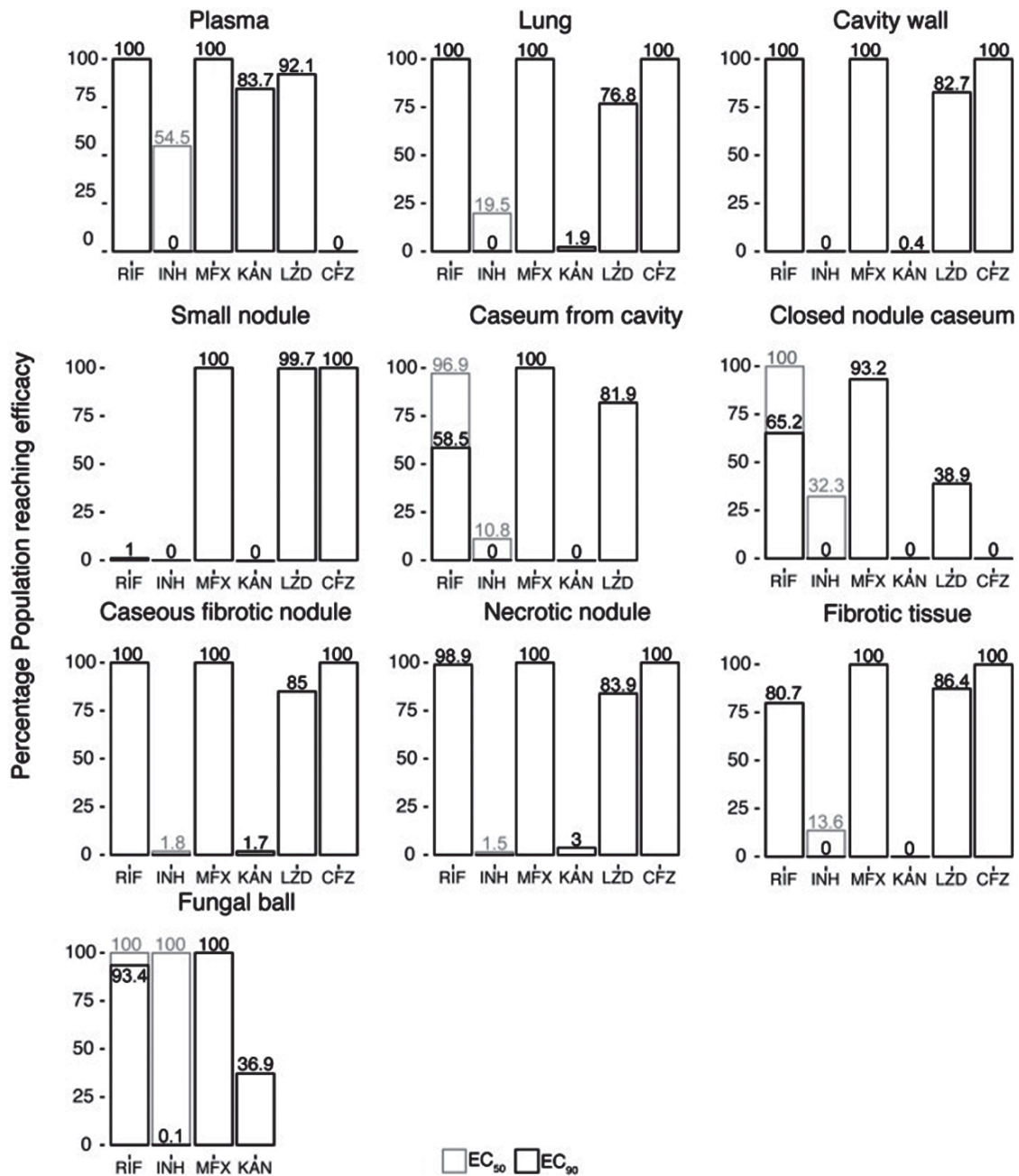


Fig 1. Prediction of drug efficacy by lesion type

Using defined critical PK/PD exposure values, a population of 1,000 simulated patients were defined as reaching efficacy or not from their PK simulations. The percentage of those reaching efficacy are shown as percentage box plots to compare the drugs that are able to reach a higher ratio of efficacy in specific lesions. Black boxes represent the percentage population reaching EC_{90} , and if available, gray boxes represent the percentage population able to reach EC_{50} . EC_{90} , 90 % maximal effective concentrations; EC_{50} , 50 % maximal effective concentrations; PK/PD, pharmacokinetic/pharmacodynamics.

cavity caseum [29], additional population PK/PD distributions were simulated using caseum-specific minimum bactericidal concentration MBC_{90} (Cas MBC_{90}) as the PD parameter to capture the drugs' killing potential in the caseous core of necrotic lesions. None of the drugs were able to reach full efficacy in this hard-to-treat lesion, and MFX was the only drug to show efficacy for 31 % of the simulated population.

Implementation of the established clinical model into interactive research and clinical in silico tool

An online tool for the established model was developed to simulate different doses and schedules for each of the 7 drugs in each specific lesion for any user-entered MIC. This interactive tool can generate critical knowledge essential for drug treatment and regimen optimization in a clinical trial

ЗАРУБІЖНИЙ ДОСВІД

setting by highlighting those patients at lower exposure that are at risk of treatment failure and stratifying patients with and without cavity. The web app is hosted at <http://saviqlab.org/tb-lesion/>, with snapshots of 1 panel shown in Fig 2.

Discussion

We have described and modeled the penetration of 7 first- and second-line TB drugs in 9 different lesion types from clinically resected lung samples. The population PK and tissue distribution model successfully captured the data and observed variance.

Overall, MFX, LZD, and RIF achieved the best coverage across lesion types relative to published MIC values. Our MFX results are aligned with a recent study by Kempker and colleagues, who measured free-cavitary MFX concentrations between 1 and 6 $\mu\text{g/mL}$ approximately 2 h after drug administration [30]. In our simulations, to explore caseum-specific MBC (8 $\mu\text{g/mL}$ for RIF and 2 $\mu\text{g/mL}$ for MFX), RIF and MFX were remarkably the only 2 study drugs that could reach the concentrations required to kill 90 % of nonreplicating *Mtb* bacilli in caseum [22]. However, despite its good cidal activity in caseum, MFX does leave a substantial population of persisters behind [22]; this could explain its lack of sterilizing activity. Considering the disappointing results of the REMoxTB and RIFAQUIN trials, in which MFX failed to shorten TB chemotherapy when substituted for either INH or ethambutol in the first-line treatment of DS-TB [31,32], more studies into lesion-focused penetration and activity could guide better decision-making for regimen and trial designs. In addition to MFX's poor sterilizing activity, Drusano and colleagues demonstrated an antagonism between RIF and MFX against nonreplicating bacilli in the hollow-fiber system [33]. Additionally, there is a significant and clinically relevant drug–drug interaction between RIF and MFX, reducing MFX levels up to 40 %, which would require dose adjustment, but is often not implemented due to QT

prolongation concerns [34]. In light of these observations, our results suggest that the clinical utility of MFX may be maximized in a regimen that does not include rifamycin.

None of the drugs evaluated could reach their respective PK/PD targets in 100 % of patients with closed caseum nodules. The best outcome was seen with MFX at 93.2 % and RIF at 65.2 %. CFZ reached adequate exposure in all cellular lesion types and lesion compartments, for which PK/PD modeling indicates it contributes to regimen efficacy in a major way, except for cavity caseum, for which CFZ failed to meet target attainment. This suggests that CFZ should always be paired with TB drugs that can reach and kill bacterial populations residing in necrotic lesion compartments. This could include RIF, MFX, or LZD, but care should be taken to ensure that patients are not resistant to RIF if CFZ is used as a second-line drug. Considering these outcomes, RIF-MFX-CFZ with or without LZD could potentially be the best treatment regimen to treat the majority of patients with diverse lesions. A stratified treatment approach based on the lesion profiles of patients could also be useful, for which patients with noncavitary TB and limited pathology could be adequately treated with a short course regimen containing CFZ. Our study offers further rationale for use of stratified medicine approaches in TB care for which the right treatment as well as the right dose could be matched with the right patient to ensure optimal treatment for all patients.

INH showed poor overall distribution and did not reach any PK/PD targets. In our cohort, the majority of the patients were fast acetylators (11 out of 15), resulting in very low plasma levels in a majority of the patients, which could skew the lesion results toward very low levels. Considering these results, and based on our simulations, INH may not perform so poorly in other regions of the world where distribution of acetylator status is more balanced. Administration of high-INH dose could also help; for example, based on our

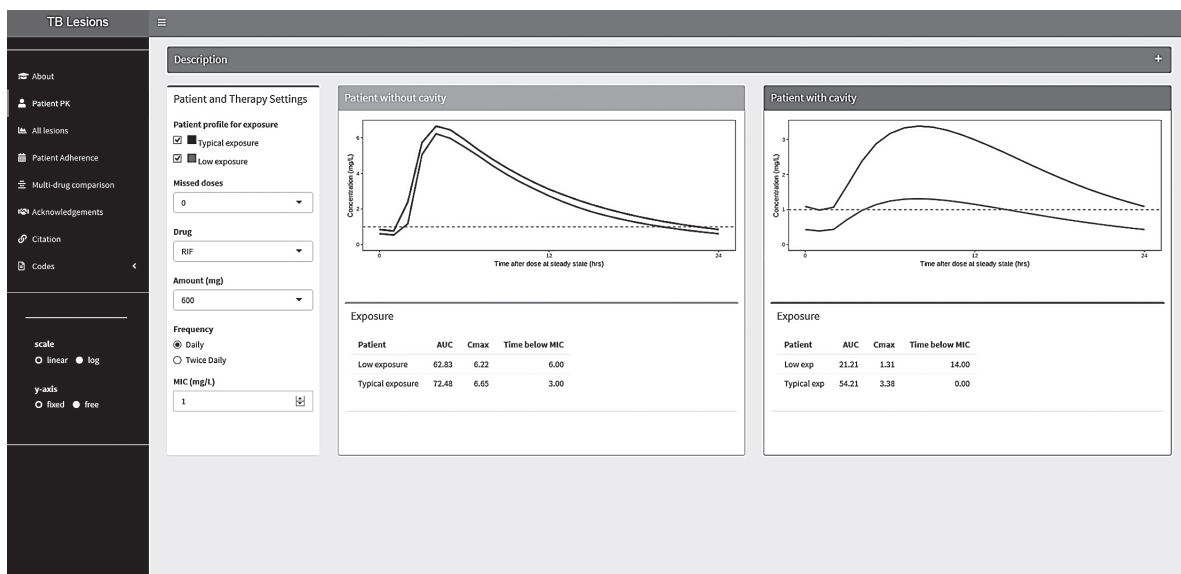


Fig 2. Interactive web application

A page of the web app is shown that displays 2 scenarios of a patient presenting with or without cavity. The user can investigate the patient's exposure distribution, dosing, and microbiology properties.

І ЗАРУБІЖНИЙ ДОСВІД

simulations, administration of a daily 15-mg/kg dose in slow acetylators would result with some coverage in caseum from cavity and closed nodule caseum.

KAN was another drug that performed poorly, and considering aminoglycoside cross-resistance, serious side effects, and a less favorable view of injectable drugs for TB treatment due to adherence problems, the use of KAN proves to be limited and of little value, as has recently been confirmed in new WHO Rapid Communication: Key changes to treatment of multidrug- and rifampicin-resistant tuberculosis (MDR/RR-TB) Guideline [35,36].

LZD showed good penetration into all lesions, confirming that LZD remains an excellent drug choice for TB treatment, as recently observed in clinical trials or extensively drug-resistant TB (XDR-TB) from an efficacy standpoint [37]. Use of LZD will remain limited by its toxicities, namely anemia and neuropathy, and an optimal risk/benefit ratio is yet to be determined.

For all of our simulations, we have used general MIC targets as recommended by standardized European Committee on Antimicrobial Susceptibility Testing/Clinical & Laboratory Standards Institute (EUCAST/CLSI) methodology as well as literature [15,16]. The accuracy in MIC measurements and any uncertainties around these values would carry over to the simulations. More precise assessment of MIC, as recently recommended by Alland and colleagues, would benefit accuracy and precision of our simulations [38]. For this reason, our interactive tool allows the MIC of drugs to be adjusted by the user as new mycobacterial targets become available.

Our patient population failed their initial TB treatment, and one of the potential reasons could be overall low drug levels leading to suboptimal therapy. Low drug exposures could be a consequence of nonadherence, reduced bioavailability, or increased clearance, all leading to suboptimal drug levels compared to the general population. However, the plasma PK parameter estimates from our models were within range of reported literature values. A recent patient-pooled analysis showed that HIV seropositivity, low BMI, adherence, baseline burden, and cavitation were all significant risk factors for treatment failure [39]. Both cavitation and adherence would lead to reduced levels in the cavities despite satisfactory plasma levels. Indeed, as shown in our study, drug levels in the cavities were very much reduced, which can explain why cavitation is an important risk factor for poor treatment response and might contribute to failing treatment in our cohort. Indeed, all patients had TB lesions so significant and diverse that they required lung resection as treatment. Our study offers a pharmacological and mechanistic explanation as to why cavitation indeed is such an important risk factor for TB outcome.

Most of the TB drugs show large between-patient variability in plasma drug levels. To explore the impact of PK variability, we have conducted population simulations to explore how patients with very low plasma levels would perform in terms of lesion PK and PK/PD target attainment, providing further rationale for the likelihood of poor clinical response due to suboptimal PK. First- and second-line drugs showed suboptimal concentrations in the lesions of these patients, especially cavity caseum and closed nodule caseum, in agreement with the poor prognostics associated with cavitary TB [39,40]. This also further suggests that a majority of the TB drugs might not be used at their optimal dose.

Emergence of resistance is prevalent in cavities, and different resistant isolates have been retrieved from different cavities of the same patient [41,42], pointing toward diverging resistance evolution, depending on lesion-specific context (bacterial load, drug tolerance of local populations [22], and fluctuating drug levels). Such lesion-specific acquired resistance is consistent with suboptimal penetration of a subset of the TB drugs in nonvascularized cavity caseum [7,9,43,44]. Our results, together with the recently demonstrated correlation between sub-breakpoint MIC and relapse [38], point in the direction of spatial and temporal windows of de facto monotherapy for which only one drug is present at adequate (i. e., above the concentration required to inhibit and/or kill local bacterial populations) concentrations during a significant portion or all of the dosing interval.

The limitations of this study include the relatively small sample size and the fact that individual tissue samples could only be taken at one time point for each patient, which is the time of the resection surgery. An additional limitation is that only one subject was at steady state for RIF. While a nonlinear mixed effects approach is useful to evaluate sparse data sets, RIF estimates did not capture the high caseum retention times observed in this specific patient [45], indicating that steady-state exposure of RIF could have been underestimated in the current model; however, any such interpretation is limited given this observation in only one patient. Further, all subjects were under anesthesia at the time of lung resection, and this could have affected drug distribution, metabolism, and elimination. The surgical procedure itself also led to 3 distinct types of lesions, namely vascular, avascular, and mixed lesion. For vascular and mixed lesions, vascular tissue and/or spill-over blood from surgery could potentially affect the final concentrations measured; however, this is likely to be negligible due to the pulmonary artery being clamped during the procedure and the tissues briefly rinsed. Finally, patients underwent lung resection due to failing their TB treatment, which may have selected for subjects that had suboptimal lesion-specific drug exposure and introduced a bias in the type of lesions present.

In conclusion, our results suggest that target attainment is both lesion and drug specific. This suggests that the current paradigm, according to which all patients receive the same regimen at the time of TB diagnosis, could be revisited. The results show that cavities and lesions that contain caseum are the most difficult to treat, as their drug levels often do not reach adequate levels over the course of treatment. It is therefore important to take special precautions when treating patients with cavitation and monitor their outcomes closely. Stratifying patients based on disease extent, lesion types, and individuals' drug-susceptibility profiles, followed by the rational selection of a tailored drug regimen, may lead to more adequate drug coverage of bacterial subpopulations residing in TB lesions. To that end, we provide an interactive tool that is able to estimate lesion-focused drug levels following any dose and schedule for these 7 drugs with the aim to support smarter design of regimens for clinical trial settings.

Стаття друкується скорочено. Повна версія статті та список літератури знаходяться в редакції та можуть бути надані за запитом.

The article is published in a cut version. The full material from the original article and literature are available on demand.